Stochastic background of gravitational waves generated by a cosmological population of young, rapidly rotating neutron stars

Valeria Ferrari,[1] Sabino Matarrese[2] and Raffaella Schneider[1]

[1]*Dipartimento di Fisica 'G. Marconi', Universitá degli Studi di Roma, 'La Sapienza' and Sezione INFN ROMA1, piazzale Aldo Moro 5, 00185 Roma, Italy*
[2]*Dipartimento di Fisica 'Galileo Galilei', Universitá degli Studi di Padova and Sezione INFN PADOVA, via Marzolo 8, 35131 Padova, Italy*

ABSTRACT

We estimate the spectral properties of the stochastic background of gravitational radiation emitted by a cosmological population of hot, young, rapidly rotating neutron stars. Their formation rate as a function of redshift is deduced from an observation-based determination of the star formation history in the Universe, and the gravitational energy is assumed to be radiated during the spin-down phase associated with the newly discovered r-mode instability. We calculate the overall signal produced by the ensemble of such neutron stars, assuming various cosmological backgrounds. We find that the spectral strain amplitude has a maximum $\approx (2-4) \times 10^{-26}$ Hz$^{-1/2}$, at frequencies $\approx (30-60)$ Hz, while the corresponding closure density, $h^2 \Omega_{GW}$, has a maximum amplitude plateau of $\approx (2.2-3.3) \times 10^{-8}$ in the frequency range $(500-1700)$ Hz. We compare our results with a preliminary analysis done by Owen et al., and discuss the detectability of this background.

Key words: gravitation – stars: formation – stars: neutron.

1 INTRODUCTION

In the last two years, a series of investigations on the perturbations of rotating relativistic stars have revealed the existence of a class of r-modes that are unstable as a result of the emission of gravitational radiation (Andersson 1998; Friedman & Morsink 1998; Lindblom, Owen & Morsink 1998). This gravitationally driven instability is of considerable importance because it has a number of interesting astrophysical implications. For instance, it determines a spin-down of newly born neutron stars to periods closer to the initial periods inferred for ms pulsars. Moreover, as the star spins down, energy equivalent to ≈ 1 per cent of a solar mass is emitted in gravitational waves, making the process a very interesting source for gravitational-wave detection (Owen et al. 1998; Andersson, Kokkotas & Schutz 1998a).

In this paper we study the stochastic background of gravitational waves contributed by a cosmological population of hot, young, rapidly rotating neutron stars with a small initial excitation in the $l = 2$ r-mode. A rough estimate of the spectrum of this background radiation has recently been given by Owen et al. (1998), assuming a comoving number density of neutron star births which is constant in the range $0 < z < 4$ and zero at earlier times.

Here we present a more complete analysis, which derives the neutron star birth rate as a function of redshift from an observation-based determination of the star formation density evolution (Madau, Pozzetti & Dickinson 1998a) within three different cosmological background models. Thus, the present investigation relies on a source rate which correctly accounts for the observed strong luminosity evolution of star-forming galaxies

between $z = 0$ and $z = 1 - 2$ (Lilly et al. 1996; Connolly et al. 1997). Using a similar approach, the gravitational background emitted by an ensemble of stellar mass black holes has been recently computed by Ferrari, Matarrese & Schneider (1999, Paper I, this issue).

The plan of the paper is as follows. In Section 2 we calculate the universal rate of neutron star formation; in Section 3 we briefly introduce the adopted model of gravitational-wave emission by an unstable rapidly rotating neutron star, closely following the recent analysis by Owen et al. (1998); in Section 4 we estimate the overall stochastic background produced by the ensemble of such sources throughout the Universe and calculate the total duty cycle of the process; Section 5 contains a brief analysis of the detectability of such a background, while conclusions are drawn in Section 6.

2 THE RATE OF NEUTRON STAR FORMATION IN THE UNIVERSE

Type II and Type Ibc supernovae are fuelled by the gravitational contraction of their cores (e.g. Ruiz-Lapuente, Canal & Isern 1997). Numerical studies have shown that single stars with masses between 8 and $20 M_\odot$ form iron cores with masses near the Chandrasekhar limit (e.g. Timmes, Woosley & Weaver 1996). Thus, there is universal agreement that these stars leave neutron star remnants. The fate of stars with masses greater than $20 M_\odot$ is less certain and depends on the iron core masses formed and on the effect of fall-back during the explosion (cf. Woosley & Weaver 1995; Woosley & Timmes 1996).
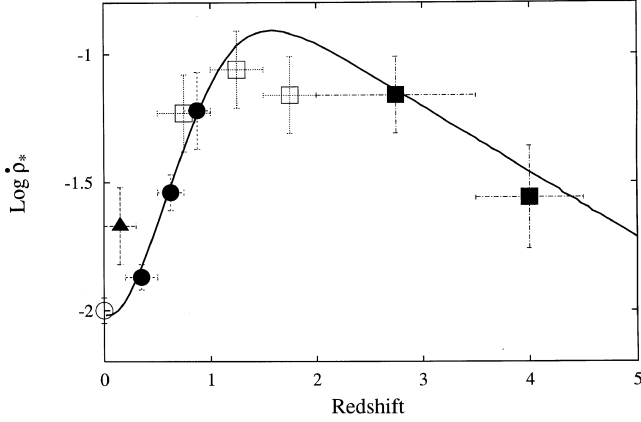
Figure 1. Evolution of the SFR density (M$_\odot$ yr^{-1} Mpc^{-3}) for $\Omega_0 = 1$, ($\Lambda = 0$), $h = 0.5$ and a Salpeter IMF. The data points are taken from Gallego et al. (1995) (empty dot), Treyer et al. (1998) (filled triangle), Lilly et al. (1996) (filled dots), Connolly et al. (1997) (empty squares) and the HDF (Madau et al. 1996) (filled squares). The solid line represents the SFR density evolution assumed in the present analysis. The fit has been kindly provided by P. Madau.

For the calculations to follow, we assume that stars with masses between 8 and 25 M$_\odot$ give rise to neutron stars. However, we will also investigate the effect of an upper mass cut-off of $\sim$20 M$_\odot$.

The number of neutron stars formed per unit time within the comoving volume out to redshift z is given by (Ferrari et al. 1999)

$$R_{\rm NS}(z) = \int_0^z \dot\rho_*(z') \, \frac{{\rm d}V}{{\rm d}z'} \, {\rm d}z' \int_{8\,{\rm M}_\odot}^{25\,{\rm M}_\odot} \Phi(M) \, {\rm d}M. \tag{1}$$

Here $\dot\rho_*(z)$ is the star formation rate density (mass of gas that goes into stars per unit time and unit comoving volume), $\Phi(M)$ is the initial mass function (IMF), and ${\rm d}V/{\rm d}z$ is the comoving volume element.

Following Madau et al. (1998a), we model the star formation evolution from the recent collection of UV–optical observations of star forming galaxies out to redshifts $\sim$4$-$5, by assuming a Salpeter IMF,

$$\Phi(M) \propto M^{-(1+x)}, \qquad \text{with } x = 1.35, \tag{2}$$

normalized through the relation

$$\int_{0.1\,{\rm M}_\odot}^{125\,{\rm M}_\odot} M \, \Phi(M) \, {\rm d}M = 1. \tag{3}$$

The star formation history is plotted in Fig. 1 for a flat cosmology with vanishing cosmological constant and $h = 0.5$ (here h is the Hubble constant, H_0, in units of 100 km s^{-1} Mpc^{-1}). The star formation rate rises sharply from its local value to a peak at $z \sim 1.5$, only to fall again out to $z \sim 4$. This behaviour indicates that the bulk of the stellar population was assembled in the redshift range $1 \lesssim z \lesssim 2$. This is consistent with the indications of QSO absorption lines and metallic clouds observations (Lanzetta, Yahil & Fernandez-Soto 1996; Pei & Fall 1995) and with the predictions of semi-analytic models for a broad class of hierarchical clustering cosmologies (Baugh et al. 1998). A thorough review of the current state of observations of the star formation history of field galaxies is given in Ellis (1997).

A summary of the relevant aspects for the present analysis is given in Ferrari et al. (1999).

The predictions for the rate of core-collapse supernovae are in good agreement with the observed local values (Cappellaro et al. 1997). At $z > 1$, the detection of Type II events must await future

Table 1. Cosmological parameters adopted in the three backgrounds considered.

Model	Ω_M	Ω_Λ	h
A	1	0	0.5
B	0.3	0.7	0.6
C	0.4	0	0.6

experiments, such as the *Next Generation Space Telescope* (Madau, Della Valle & Panagia 1998b).

Here we shall only stress that one major source of uncertainty in the interpretation of the data points in Fig. 1 is the effect of dust extinction. Even a small amount of dust in primeval galaxies can significantly attenuate the UV luminosity and re-radiate it in the far-IR, thus leading to a potentially serious underestimate of the star formation activity. Dust correction factors are still very uncertain, mainly because of the unknown shape of the dust UV-extinction law (Pettini et al. 1997). The model for the global SFR evolution presented in Fig. 1 assumes an extinction law similar to that which applies to stars in the Small Magellanic Cloud (SMC) and an amount of dust which results in an upwards correction of the comoving UV luminosity by a factor 1.4 at 2800Å and 2.1 at 1500Å (Madau et al. 1998a). Recent near-infrared observations of a galaxy at $z = 4.92$ have given evidence that absorption by dust is important up to redshifts of $\sim$5 (Soifer et al. 1998). Similarly, analysis of the *Infrared Space Observatory* (*ISO*) data has shown a significant departure from the UV–optically derived SFR evolution at $z > 2$ (Rowan-Robinson et al. 1997).

This may seem a serious caveat for the present investigation. However, this is not necessarily the case because the extragalactic astrophysical gravitational-wave backgrounds prove to be mainly contributed by low-to-intermediate redshift sources. High redshift sources play a negligible role because the energy flux emitted by each source decreases as the inverse of the squared luminosity distance. On the other hand, if an upward correction of the UV–optically derived SFR density is required at $z \approx 1.5$, as suggested by a recent detection of the infrared background by the Diffuse Infrared Background Experiment (DIRBE) and the Far Infrared Absolute Spectrometer (FIRAS) on board the *Cosmic Background Explorer* (*COBE*) satellite (Dwek et al. 1998), this would result in an upward correction of roughly the same amplitude on our gravitational-wave background predictions.

We have evaluated equation (1), below, for three sensible cosmological models (e.g. Baugh et al. 1998), namely a flat geometry with vanishing cosmological constant, an open background and a flat low-density model (see Table 1).

For a general background, the comoving volume element is related to z through
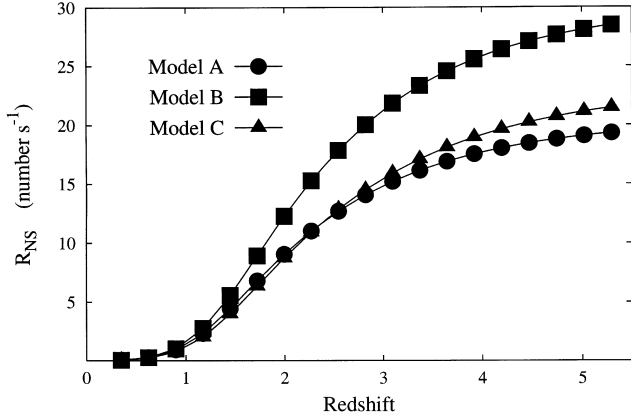
$$ {\rm d}V = 4\pi \left(\frac{c}{H_0}\right) r^2 \, \mathcal{F}(\Omega_M, \Omega_\Lambda, z) \, {\rm d}z, \tag{4}$$

where H_0 is the Hubble constant and

$$ \mathcal{F}(\Omega_M, \Omega_\Lambda, z) \equiv \frac{1}{\sqrt{(1+z)^2 (1 + \Omega_M z) - z(2+z)\,\Omega_\Lambda}}. \tag{5}$$

In equation (4), r is the comoving distance

$$ r = \frac{c}{H_0 \sqrt{\Omega_\kappa}} S\left(\sqrt{\Omega_\kappa} \int_0^z [(1+z')^2 (1 + \Omega_M z') - \right. $$
$$ \left. z'(2+z')\,\Omega_\Lambda]^{-1/2} \, {\rm d}z' \right) \tag{6}$$

Figure 2. Evolution of the rate of neutron star formation for three different cosmological scenarios.

and the function S has the following expression (Perlmutter et al. 1997):

$$\Omega_M + \Omega_\Lambda > 1 \quad S(x) = \sin(x), \quad \Omega_\kappa = 1 - \Omega_M + \Omega_\Lambda, \quad (7)$$
$$\Omega_M + \Omega_\Lambda < 1 \quad S(x) = \sinh(x) \quad \Omega_\kappa = \Omega_M + \Omega_\Lambda - 1,$$
$$\Omega_M + \Omega_\Lambda = 1 \quad S(x) = x \qquad \Omega_\kappa = 1.$$

Consistently, the SFR history shown in Fig. 1 needs to be properly rescaled in order to account for the cosmological background dependence of both the luminosity distance and the comoving volume within each redshift bin.

Using equation (4), we have evaluated the function $R_{NS}(z)$ defined in equation (1) for the three cosmological models, and the results are shown in Fig. 2.

It should be mentioned that the evaluation of the rate of neutron star formation, based on the UV–optically estimated star formation rate evolution $\dot{\rho}_*(z)$, and on an assumed universal IMF, is largely independent of the specific IMF adopted (Madau 1998). In fact, the stars which contribute most to the UV–optical luminosity are the most massive ones which, in turn, are those that at the end of their evolution give rise to core-collapse supernovae.

The total number of supernova explosions per unit time leaving behind a neutron star is given in Table 2 for the considered cosmological models, and for two values of the upper mass cut-off, $M_u = 25\,M_\odot$ and $M_u = 20\,M_\odot$. As a consequece of the largest number of stars having masses $< 25\,M_\odot$, the total rate of core collapses to neutron stars is a factor ~ 4 larger than that of core collapses to black holes considered in Ferrari et al. (1999).

3 GRAVITATIONAL EMISSION FROM RAPIDLY ROTATING NEUTRON STARS

In this section we shall briefly describe how the time-scale of the

Table 2. Values of the total rate of neutron stars in different cosmological scenarios and for two values of the upper progenitor mass cutoff ($20\,M_\odot$, $25\,M_\odot$).

Model	$M_u/M_\odot$	R_{NS}/(events per s)
A	25	19.5
A	20	17.6
B	25	28.7
B	20	25.9
C	25	21.7
C	20	19.6

spin-down phase and the energy spectrum of the gravitational radiation emitted during the r-mode instability have been estimated (Lindblom et al. 1998; Owen et al. 1998; Andersson et al. 1998a; Andersson, Kokkotas & Stergioulas 1998b). These quantities will be used to compute, respectively, the duty cycle and the spectral energy density of the stochastic background.

The excitation of an r-mode starts as a small perturbation of the velocity field. As the amplitude of the mode grows, non-linear hydrodynamic effects become important and eventually dominate the dynamics. Under the assumption that the star is uniformly rotating with angular velocity Ω, and by parametrizing the r-mode by its amplitude α, the star can be considered as a system having only two degrees of freedom, Ω and α. In this simple model, the total angular momentum for the $\ell = 2$ r-mode can be shown to be

$$J(\Omega, \alpha) = \left(\tilde{I} - \frac{3}{2} \tilde{J} \alpha^2 \right) \Omega M R^2 , \qquad (8)$$

where

$$\tilde{I} = \frac{8\pi}{3MR^2} \int_0^R \rho \, r^4 \, dr \quad \text{and} \quad \tilde{J} = \frac{1}{MR^4} \int_0^R \rho r^6 dr , \qquad (9)$$

and the rotational energy is

$$E \approx J(\Omega, \alpha)\Omega. \qquad (10)$$

Following Owen et al. (1998), we shall consider a Newtonian model of a neutron star composed of a fluid with a polytropic equation of state, $p = k\rho^2$, with k chosen so that $M = 1.4\,M_\odot$ and $R = 12.53$ km. For this model, $\tilde{I} = 0.261$ and $\tilde{J} = 1.635 \times 10^{-2}$. It should be noted that $\tilde{I}$ and $\tilde{J}$ depend only on the chosen polytropic index.

The evolution of the angular momentum of the star is determined by the emission of gravitational waves, which couple to the r-modes through the current multipoles, primarily that with $l = m = 2$. For this mode, the frequency of the emitted gravitational radiation is $\nu = (2/3\pi)\,\Omega$. The evolution of Ω and α during the phase in which α is small, can be determined from the standard multipole expression for angular momentum loss, and from the energy loss arising from the gravitational emission and the dissipative effects induced by the bulk and shear viscosity. In this phase, Ω is nearly constant and α grows exponentially. After a short time, which Owen et al. estimate to be of order 500 s, the amplitude of the mode becomes close to unity and non-linear effects saturate and halt further growth of the mode. This phase lasts for approximately 1 yr, during which the star loses angular momentum radiating approximately 2/3 of its initial rotational energy in gravitational waves, up to a point where the angular velocity and the temperature are so low that the r-mode ceases to be unstable. Viscous forces and gravitational radiation damp out the energy left in the mode, and the star slowly reaches its final equilibrium configuration.

Since gravitational radiation is emitted over such a long time interval, the background contributed by neutron stars is continuous. In fact, the total duty cycle for this process is

$$D = \int_0^\infty dR_{NS}(z)\,\bar{\tau}_{NS}(1+z) \sim 10^9. \qquad (11)$$

It has been suggested that if the proton fraction in the star is sufficiently large to make the direct URCA process possible, the star would cool in a much shorter time, $\bar{\tau}_{NS} \approx 20$ s. However, if this were the case, the duty cycle would still be $\gg 1$ ($D \approx 10^2$) and the resulting background would still be continuous.

It is known that the angular velocity of a rotating star cannot exceed the Kepler frequency Ω_K at which mass shedding at the stellar equator makes the star unstable. A reasonable approximation

for this limiting frequency is

$$\Omega_K \approx C \sqrt{\frac{M}{M_\odot} \left(\frac{10\,\text{km}}{R}\right)^3} , \tag{12}$$

where $C \approx 7.8 \times 10^3\,\text{s}^{-1}$ (Friedmann, Ipser & Parker 1989), and M and R refer to the mass and radius of the corresponding non-rotating star. Following Owen et al., we shall assume that neutron stars are born with angular velocity close to the maximum value Ω_K, and have a rotational kinetic energy

$$E_K \approx J(\Omega_K; \alpha)\,\Omega_K = \left(\tilde{I} - \frac{3}{2}\,\tilde{J}\alpha^2\right) M R^2 \Omega_K^2 . \tag{13}$$

In the non-linear saturation phase, where most of the gravitational radiation is emitted, $\alpha \approx 1$. Since in this simple model approximately 2/3 of the rotational energy of the star is radiated in gravitational waves, the expression of the energy spectrum can be approximated as follows

$$\frac{dE_{GW}}{d\nu} \approx \frac{4}{3}\,E_K\,\frac{\nu}{\nu_{max}^2} , \tag{14}$$

where

$$\nu_{max} = (2/3\pi)\Omega_K . \tag{15}$$

The r-mode instability ceases to be effective for some value of the rotational frequency Ω_c, which corresponds to the final spin period, and which is associated to a gravitational emission frequency

$$\nu_{min} = (2/3\pi)\Omega_c . \tag{16}$$

Ω_c can be determined by solving the equation $1/\tau(\Omega_c) = 0$, where τ is the total dissipation time-scale which can be decomposed as a sum of the damping times associated to the gravitational emission, to the shear and to the bulk viscosity. $\tau(\Omega_c)$ is clearly a function of the temperature of the star, and it has been shown that the r-mode instability operates only in hot neutron stars ($T > 10^9$ K). Below 10^9 K, superfluidity and other non-perfect fluid effects become important and the damping arising from viscosity dominates with respect to the destabilizing effect of the gravitational radiation. To be consistent with the analysis by Owen et al. (1998), we shall adopt a value of $\Omega_c \approx 566$ Hz for the final angular velocity which corresponds to a final spin period of ≈ 11 ms and to $\nu_{min} \approx 120$ Hz.

The qualitative picture that arises from this simple model is believed to be sufficiently reliable, even though various uncertainties and approximations might affect the quantitative results for the initial rotation of the star after collapse, for the spin-down time-scales as well as for the final rotation period (Andersson et al. 1998a). Thus, it will be interesting to evaluate the effects that different values of ν_{max}, E_K and ν_{min} have on our main conclusions.

4 SPECTRAL PROPERTIES OF THE STOCHASTIC BACKGROUND

In order to evaluate the spectral energy density of the stochastic background produced by the spindown radiation from newly born neutron stars, we need to know how the flux emitted by a single source at redshift z would be observed today, and convolve it with the differential rate of the sources $dR_{NS}(z)$ as in Ferrari et al. (1999).

The average energy flux per unit frequency emitted by a single neutron star at cosmological redshift z is

$$f(\nu^{obs}) = \frac{1}{4\pi d_L(z)^2}\left(\frac{dE_{GW}}{d\nu}\right)^{obs} , \tag{17}$$

where ν^{obs} is the frequency at which the radiation would presently be observed. The energy flux $f(\nu^{obs})$ can be evaluated by making use
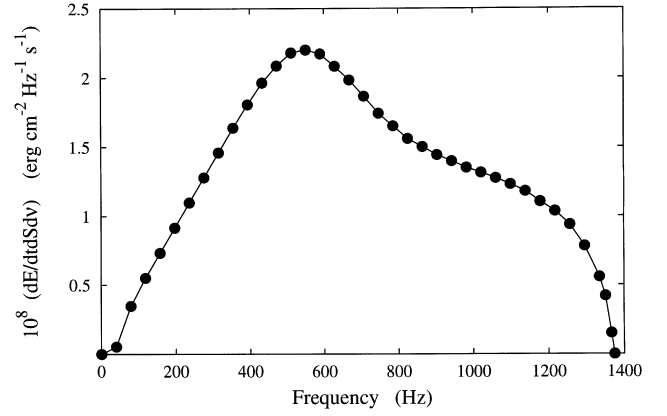
Figure 3. The spectral energy density ($dE/dSdtd\nu$) is plotted as a function of the observational frequency for the cosmological background corresponding to model A (see Table 1).

of equation (14) suitably redshifted as

$$f(\nu^{obs}) = \frac{E_K}{3\pi}\,\frac{\nu^{obs}}{(\nu_{max}^{obs})^2}\,\frac{1}{(1+z)\,d_L(z)^2} , \tag{18}$$

where

$$\frac{\nu_{min}^{em}}{1+z} \leqslant \nu^{obs} \leqslant \frac{\nu_{max}^{em}}{1+z} , \tag{19}$$

and $d_L(z) = (1+z)\,r$ is the luminosity distance, which depends on the cosmological model as indicated in equation (7). Thus, the spectral energy density of the produced background is

$$\frac{dE_{GW}}{dt dS d\nu} = \int_0^\infty f(\nu)\,dR_{NS}(z) , \tag{20}$$

where the differential rate of sources is given by

$$dR_{NS}(z) = \dot{\rho}_*(z)\,\frac{dV}{dz}\left[\int_{8\,M_\odot}^{25\,M_\odot}\Phi(M)\,dM\right]dz . \tag{21}$$

(see equation 1). From the spectral energy density, the corresponding values of the closure energy density of gravitational waves,

$$\Omega_{GW}(a, \nu_{obs}) = \frac{\nu_{obs}}{c^3 \rho_{cr}}\,\frac{dE}{dt dS d\nu} , \tag{22}$$

where $\rho_{cr} = 3H_0^2/8\pi G$, and of the spectral strain amplitude

$$\sqrt{S_h(\nu_{obs})} = \left(\frac{2G}{\pi c^3}\,\frac{1}{\nu_{obs}^2}\right)^{1/2}\left(\frac{dE}{dt dS d\nu}\right)^{1/2} \tag{23}$$

can be derived.

In Figs 3 and 4 we plot the spectral energy density and the strain amplitude for the flat background with zero cosmological constant corresponding to model A (see Table 1). The effect of a varying cosmological background is negligible on both the spectrum and the strain amplitude. In fact, the amplification of the rate at high redshifts shown in Fig. 2 for the models B and C, is mostly suppressed by the inverse squared luminosity distance dependence of the single source spectrum (see equation 18) for the same models. Conversely, the closure density exhibits a more evident dependence on the Hubble constant, as shown in Fig. 5, where we have considered only model A and B because the dependence on the other cosmological parameters (namely Ω_M and Ω_Λ) is negligible.

The estimate of the intensity of the stochastic background also depends on the chosen values of ν_{min} and ν_{max}. We have repeated our calculations for two values of ν_{min}, chosen so as to cover the range
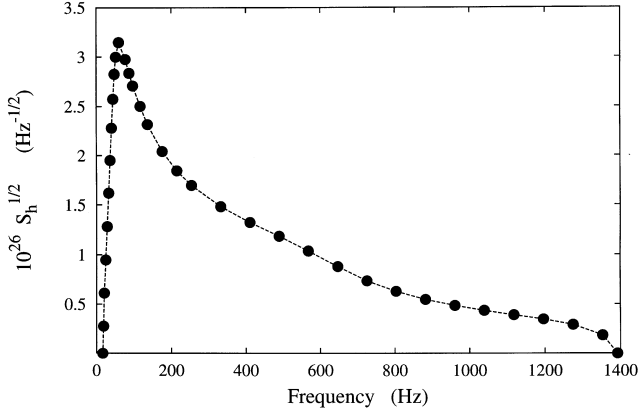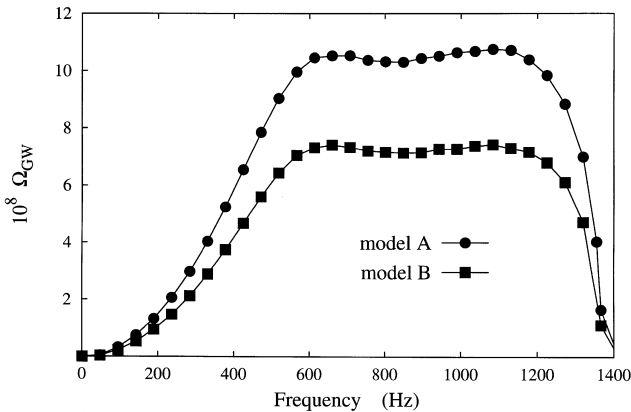
Figure 4. The spectral strain amplitude $S_h^{1/2}$ corresponding to the spectral energy density given in Fig. 3 is plotted as a function of the observational frequency.

of pulsar rotational periods, P_{in}, inferred from observations

$$\nu_{min} = \frac{4}{3} P_{in}^{-1} \,, \tag{24}$$

with P_{in} between 9 and 22.8 ms, where the upper limit is the maximum rotational period at which the r-modes are unstable (Andersson et al. 1998a). Since the strain amplitude is sensitive mainly to the low-frequency region of the spectrum, because of the factor ν_{obs}^{-1} in equation (23), a decrease of ν_{min} determines an increase of the peak amplitude and shifts its location towards lower frequencies, as shown in Fig. 6.

The value of ν_{max} depends on Ω_K which, in turn, depends on the mass and radius of the star, as shown in equations (15) and (12). The plots shown in Figs 3, 4 and 5 were obtained by assuming $M = 1.4 \, M_\odot$ and $R = 12.53$ km. In reality, the possible radii for rotating neutron stars range from 10 to 15 km. Therefore, since the dependence of Ω_K on the mass is less significant than its dependence on the radius, we have computed the strain amplitude and the closure density by considering $M = 1.4 \, M_\odot$, and changing the radius to $R = 10$ km and to $R = 15$ km. The effect of reducing ν_{max}, i.e. of increasing the radius, is that of narrowing the interval of frequencies over which each source contributes. Since the energy flux of a single event does not depend on Ω_K (see equation 18), this will result in an increase of the amplitude of the peak of the spectral

Figure 5. The function Ω_{GW} corresponding to the spectral energy density plotted in Fig. 3. Since the main effect on the gravitational background is a result of the change in the Hubble constant, we have plotted only two curves corresponding to an $h = 0.5$ flat model without cosmological constant and to an $h = 0.6$ flat model with a cosmological constant (see Table 1).
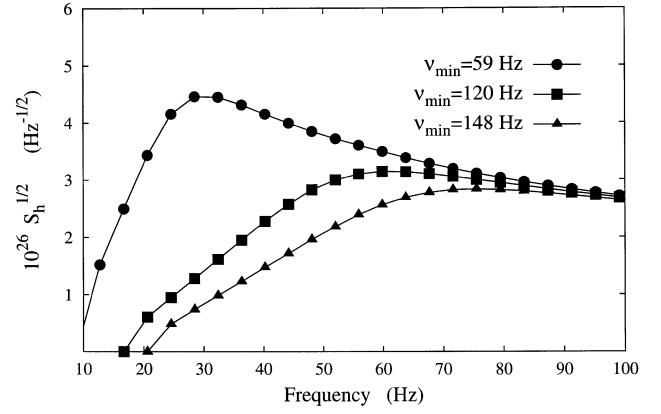
Figure 6. The spectral strain amplitude $S_h^{1/2}$ corresponding to a flat model is plotted as a function of the observational frequency for three different values of ν_{min} (see text).

energy density. This effect is amplified in the strain amplitude, which is more sensitive to low frequencies. However, it should be stressed that the increase is smaller than a factor of 2. Conversely, the closure density is more sensitive to the high-frequency contributions, and therefore the effect is the opposite. The results are shown in Figs 7 and 8.

5 DETECTABILITY

The value of the optimal signal-to-noise ratio (S/N) for L-shaped interferometers can be computed according to the formula (Allen 1997)
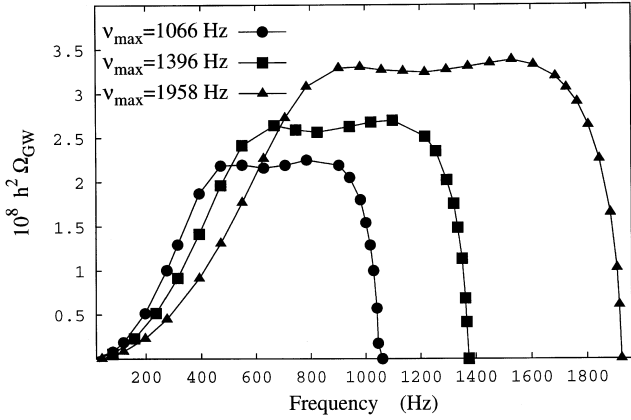
$$S/N^2 = \left[\left(\frac{9H_0^4}{50\pi^4} \right) T \int_0^\infty d\nu \, \frac{\gamma^2(\nu)\Omega_{GW}^2(\nu)}{\nu^6 S_h^{(1)}(\nu) S_h^{(2)}(\nu)} \right] \tag{25}$$

where $S_h^{(i)}$ are the spectral noise densities of two detectors operating in coincidence, and $\gamma(\nu)$ is the overlap function which takes into account the differences in their location and orientation. We shall calculate the S/N for several pairs of detectors, and for Ω_{GW} computed for a flat cosmology, $\nu_{min} = 120$ Hz, and $\nu_{max} = 1396$ Hz. We shall assume an integration time of $T = 1$ yr.

For interferometric antennas, we have computed $S_h^{(i)}$ from the expected sensitivity curves given for VIRGO (Beccaria et al. 1996) and for ADVANCED LIGO (Flanagan & Hughes 1998). The
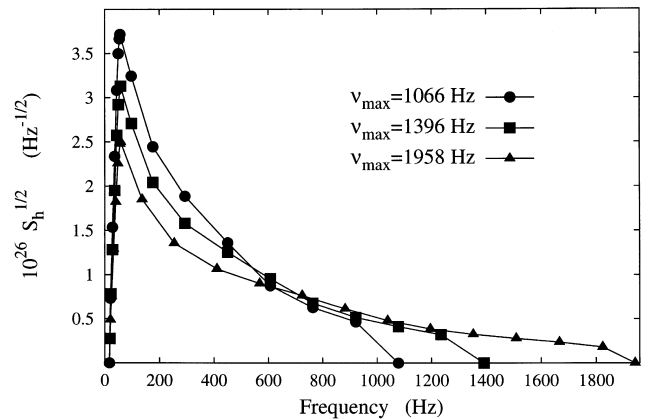
Figure 7. The spectral strain amplitude $S_h^{1/2}$ corresponding to a flat model is plotted as a function of the observational frequency for three different values of the radius and, thus, of the initial rotational period and of the total rotational energy (see text).

Figure 8. The function Ω_{GW} corresponding to the spectral strain amplitude plotted in Fig. 7.

Figure 9. A comparison with the closure density, $h^2 \Omega_{GW}$, predicted by Owen et al. (1998) is plotted as a function of the observational frequency for the cosmological background corresponding to model A.

sensitivity curve for GEO600 has been extracted from the Web site http://www.geo600.uni-hannover.de.

For VIRGO and GEO600 we find $S/N = 3.7 \times 10^{-3}$, assuming optimal orientation, and $S/N = 5.0 \times 10^{-3}$ if GEO600 is narrow-banded around 100 Hz. For two ADVANCED LIGO detectors, $S/N = 0.84$. Since the correlation of two interferometers at a distance d starts to be very poor around a frequency $\approx (70\,\mathrm{Hz})(3000\,\mathrm{km}\,d^{-1})$ (Allen & Romano 1997), two nearby detectors respond better to higher frequencies, where our predicted signal has a larger amplitude (see Fig. 8). Thus, the S/N rises to 8.5 if we consider two nearby ADVANCED LIGO (or VIRGO) interferometers at a distance of ≈ 300 km.

We have similarly investigated how interferometric and resonant detectors operating in coincidence might respond to our predicted background. The correlation of VIRGO and NAUTILUS, situated 265 km apart, gives $S/N = 3.0 \times 10^{-4}$. Assuming that a similar correlation is done with a truncated icosahedral antenna (TIGA) (Merkowitz & Johnson 1995) and a LIGO interferometer located at the same site, the resulting S/N is $\approx 1.3 \times 10^{-3}$, whereas it is $\approx 1.7 \times 10^{-3}$ if the interferometer is ADVANCED VIRGO.

Thus, the detection of this background requires two nearby interferometers with 'advanced' sensitivities, as similarly noted by Owen et al. (1998).

6 CONCLUSIONS

In this paper we have evaluated the gravitational background produced by a cosmological population of hot, young and rapidly rotating neutron stars, emitting gravitational radiation during the spin-down phase associated with the r-mode instability. The dependence of this background on the cosmological model, and on the parameters that enter into the determination of the spectrum of each single event, has been discussed. Our predictions for the spectrum, spectral strain amplitude and closure density appear to be rather insensitive to the assumed cosmological parameters. This is because the increase of the neutron star birth rate that we find in an open or a flat low-density cosmology is compensated for by the increase of the luminosity distance as a function of redshift, which suppresses the contribution of the most distant sources.

For the same reason, the uncertainties that still trouble the high-redshift tail of the SFR density evolution due to dust obscuration are not severe for our signal, as this is mainly contributed by low-to-intermediate redshift sources. Moreover, if dust obscuration
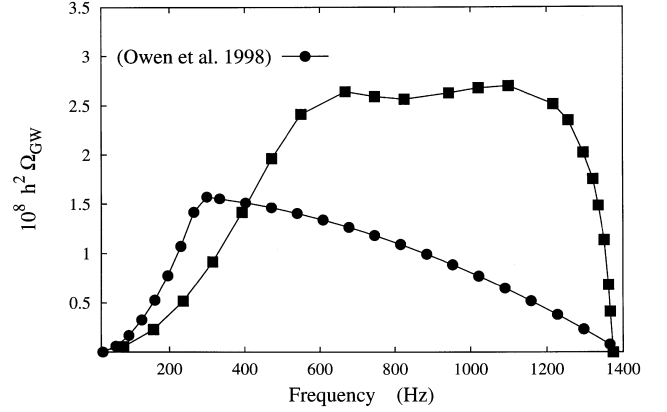
produces an upward correction of the SFR density at intermediate redshifts (i.e. around the location of the maximum), then the amplitude of $(S_h)^{1/2}$ and of Ω_{GW} will be similarly amplified at ≈ 30 and ≈ 600 Hz respectively.

We find that, within a reasonable range of values of the main parameters which characterize the energy spectrum of a single source (namely ν_{min}, ν_{max} and E_K), the spectral strain amplitude has a maximum ranging within $\approx (2-4) \times 10^{-26}\,\mathrm{Hz}^{-1/2}$ at frequencies $\approx (30-60)$ Hz, whereas the closure density, $h^2 \Omega_{GW}$, is shown to have a long plateau extending from ≈ 300 Hz up to ≈ 1700 Hz with an amplitude of $\approx (2.2-3.3) \times 10^{-8}$.

It is interesting to compare our results with those of a similar study done by Owen et al. (1998), who assume that the number of stars formed per unit comoving volume and redshift is constant in the range $0 \le z \le 4$, and zero elsewhere.

In Fig. 9 we show the closure density predicted by the present analysis and that obtained by Owen et al. The two curves exhibit quite a different high-frequency behaviour. Since the cosmological expansion shifts the frequencies towards smaller values, the high-frequency tail corresponds to closer sources, thus the difference between the two curves can be traced back to the SFR density evolution between $z = 0$ and $z \approx 1-2$. The peak at ≈ 600 Hz exhibited by our curve corresponds to $z \approx 1.3$, where we expect to have the maximum number of sources. Conversely, the maximum amplitude predicted by Owen et al. is located around 280 Hz, and corresponds to the energy emitted at maximum spin rate by a source at $z \sim 4$. Thus, their signal appears to be mostly contributed by distant sources near their maximum rotational velocity: this may be a result of the fact that they do not properly account for the luminosity distance damping, which is particularly effective for high-redshift sources. It is important to stress that in the region where cross-correlation between two LIGO interferometers can be accomplished, i.e. for $\nu < 50-60$ Hz, the signal is entirely emitted at $z > 1$, where it is important to embed the gravitational sources in the correct cosmological environment.

Both in our analysis and in the study of Owen et al., all neutron stars have been assumed to be initially rotating with an angular velocity close to the Keplerian value, while there might be a fraction of stars born with lower initial spin rate. In particular, no spin-down gravitational radiation would be emitted if the initial angular velocity of the star were too small for the instability to set in (Spruit & Phinney 1998). However, according to Andersson et al. (1998a) this is unlikely to be the generic situation, because the

angular momentum of the degenerate core required to make the star rotate with velocity Ω_K is rather small. Moreover, there is clear evidence that some pulsars were born spinning rapidly: as an example, the observed spin period for the young X-ray pulsar in the supernova remnant N157B is 16 ms, and its inferred initial spin period is estimated to be $\approx 6-9$ ms (Marshall et al. 1998).

REFERENCES

Allen B., 1997, in Marck J. A., Lasota J. P., eds, Relativistic Gravitation and Gravitational Radiation. Cambridge Univ. Press, Cambridge, p. 373
Allen B., Romano J. D., 1997, preprint (gr-qc/9710117)
Andersson N., 1998, ApJ, 502, 708
Andersson N., Kokkotas K., Schutz B. F., 1998a, ApJ, in press (astro-ph/9805225)
Andersson N., Kokkotas K., Stergioulas N., 1998b, ApJ, in press (astro-ph/9806089)
Baugh C. M., Cole S., Frenk C. S., Lacey C. G., 1998, ApJ, 498, 504
Beccaria M., Cella G., Ciampa A., Cuoco E., Curci G., Viceré A., 1996, VIRGO NOTE NTS96
Cappellaro E., Turatto M., Tsvetkov D. Y., Bartunov O. S., Pollas C., Evans R., Hamuy M., 1997, A&A, 322, 431
Connolly A. J., Szalay A. S., Dickinson M., SubbaRao M. U., Brunner R. J., 1997, ApJ, 486, L11
Dwek E. et al., 1998, ApJ, in press (astro-ph/9806129)
Ellis R. S., 1997, ARA&A, 35, 389
Ferrari V., Matarrese S., Schneider R., 1999, MNRAS, 303, 247 (Paper I, this issue)
Flanagan E. E., Hughes S. A., 1998, Phys. Rev. D, 57, 4535
Friedman J. L., Morsink S. M., 1998, ApJ, 502, 714
Friedman J. L., Ipser J. R., Parker L., 1989, Phys. Rev. Lett., 62, 3015
Gallego J., Zamorano J., Arágon-Salamanca A., Rego M., 1995, ApJ, 455, L1
Lanzetta K. M., Yahil A., Fernandez-Soto A., 1996, Nat, 381, 759
Lilly S. J., Le Févre O., Hammer F., Crampton D., 1996, ApJ, 460, L1
Lindblom L., Owen B. J., Morsink M., 1998, Phys. Rev. Lett., 80, 4843
Madau P., 1998, in D'Odorico S., Fontana A., Giallongo E., eds, ASP Conf. Ser. 148, The Young Universe: Galaxy Formation and Evolution at Intermediate and High Redshift. Astron. Soc. Pac., San Francisco, p. 289
Madau P., Ferguson H. C. C., Dickinson M. E., Giavalisco M., Steidel C. C., Fruchter A., 1996, MNRAS, 283, 1388
Madau P., Pozzetti L., Dickinson M., 1998a, ApJ, 498, 106
Madau P., Della Valle M., Panagia N., 1998b, MNRAS, 297, L17
Marshall F. E., Gotthelf E. V., Zhang W., Middleditch J., Wang Q. D., 1998, ApJ, 499, L179
Merkowitz S. M., Johnson W. W., 1995, Phys. Rev. D, 51, 2546
Owen B. J., Lindblom L., Cutler C., Schutz B. F., Vecchio A., Andersson N., 1998, Phys. Rev. D58, 084020
Pei Y. C., Fall S. M., 1995, ApJ, 454, 69
Perlmutter S. et al. (The Supernova Cosmology Project), 1997, ApJ, 483, 565
Pettini M., Steidel C. C., Dickinson M., Kellogg M., Giavalisco M., Adelberger K., 1997, in Waller W., ed., The Ultraviolet Universe at Low and High Redshifts. AIP Press, Woodbury
Rowan-Robinson M. et al. (The ISO–HDF Consortium), 1997, MNRAS, 289, 490
Ruiz-Lapuente P., Canal R., Isern J., 1997, in Ruiz-Lapuente P., Canal R., Isern J., eds, Proc. NATO Advanced Study Institute on Thermonuclear Supernovae. Kluwer, Dordrecht
Soifer B. T., Neugebauer G., Franx M., Matthews K., Illingworth G. D., 1998, ApJ, 501, L171
Spruit H., Phinney E. S., 1998, Nat, submitted (astro-ph/9803201)
Timmes F. X., Woosley S. E., Weaver T. A., 1996, ApJ, 457, 834
Treyer M. A., Ellis R. S., Milliard B., Donas J., Bridges T. J., 1998, MNRAS, 300, 303
Woosley S. E., Timmes F. X., 1996, Nucl. Phys. A, 606, 137
Woosley S. E., Weaver T. A., 1995, ApJS, 101, 181

This paper has been typeset from a T$_{E}$X/L^{A}T$_{E}$X file prepared by the author.